

Nanomachined Pyroelectric Detector with Low Thermal Conductance – Design and Concepts

Md Muztoba, Nouredine Melikechi, Mukti M. Rana
Optical Science Center for Applied Research (OSCAR) and
Department of Physics and Engineering
Delaware State University
Dover, DE, USA
mrana@desu.edu

Donald P. Butler
Nanotechnology Research and Education Center
and Department of Electrical Engineering
University of Texas at Arlington
Arlington, TX, USA

Abstract— We report the design of an uncooled pyroelectric detector utilizing a nanometer sized mesh to support the micromachined detector. The design had been optimized by using different geometry and electrodes. The thickness, width and dimension of each layer were changed to achieve the lowest thermal conductance. Ca-modified lead titanate (PCT) was employed as the thermometer in the detector. The design and performance of pyroelectric detectors has been conducted by simulating the structure with Intellisuite™. The simulated detector had spider web-like structure with each of the struts (ring) of spider web 100 nm wide. The pyroelectric detectors utilized a NiCr absorber, PCT sensing layer, Ti electrodes, Al₂O₃ structural layer to obtain lower thermal conductivity between the detector and substrate. The thermal conductance between the sensor and the substrate was found to be as low as 4.57×10^{-9} W/K.

I. INTRODUCTION

Pyroelectricity is the electrical response of a polar, dielectric material to a change in temperature. This property is presented by certain materials that exhibit an electric polarization and change in charge ΔQ , when a temperature variation ΔT is applied uniformly, and is related by the following relation,

$$\Delta Q = A\gamma\Delta T \quad (1)$$

Where, A is the area of the capacitor and γ is the pyroelectric coefficient at constant stress which can be expressed as,

$$\gamma = \frac{\partial P_s}{\partial T} \quad (2)$$

Where, P_s is the spontaneous polarization.

The heat transfer process between the pyroelectric detector and ambient is demonstrated in Fig. 1. The heat sink can be compared to the silicon substrate and the power input is the infrared (IR) radiation. The detector is represented by a thermal capacitance C_{th} , coupled via a thermal conductance

G_{th} , to a heat sink which is maintained at a constant temperature T. In the absence of the radiation input, the average temperature of the detector will also be T.

When a sinusoidally modulated heat flux is incident on the detector, solution of the heat balance equation provides the rise in temperature as [1, 2],

$$\Delta T = \frac{\eta\Phi}{G_{eff}\sqrt{1+\omega^2\tau_{th}^2}} \quad (3)$$

Where, η is the average absorption of the detector, τ_{th} is the thermal time constant, Φ is the optical flux intensity, and G_{eff} is the effective thermal conductance expressed as,

$$G_{eff} = G_{th} + G_{rad} \pm \alpha P_{bias} \quad (4)$$

Where, α is the temperature coefficient of resistance (TCR) of the thermometer and P_{bias} is the power dissipated in the bias of the detector, which is zero for pyroelectric detectors since they can operate without bias. G_{rad} is the radiative thermal conductance for a gray body, assuming the emissivity is equal to the absorptivity. Not much can be done other than material selection to reduce G_{rad} . However, materials known for low heat loss also absorb less infrared radiation, which is undesirable. This put the ultimate limit on the performance of the detector. G_{rad} can dominate for detectors with low thermal conductance (G_{th}), and bias heating should be avoided. This makes pyroelectric detector attractive since it can be operated without bias current.

There are two possible ways for thermal conduction. First, heat is lost through conduction/convection, through the atmosphere surrounding the detector thermometer, which can be minimized by vacuum packaging the detector. Second, heat is lost through thermal conduction through the supporting structure of the thermometer. Therefore, the design of the supporting structure directly impacts the thermal conductance.

Equation (1) indicates that a larger ΔT will lead to a larger ΔQ , which means a better detection of radiation. However, (3)

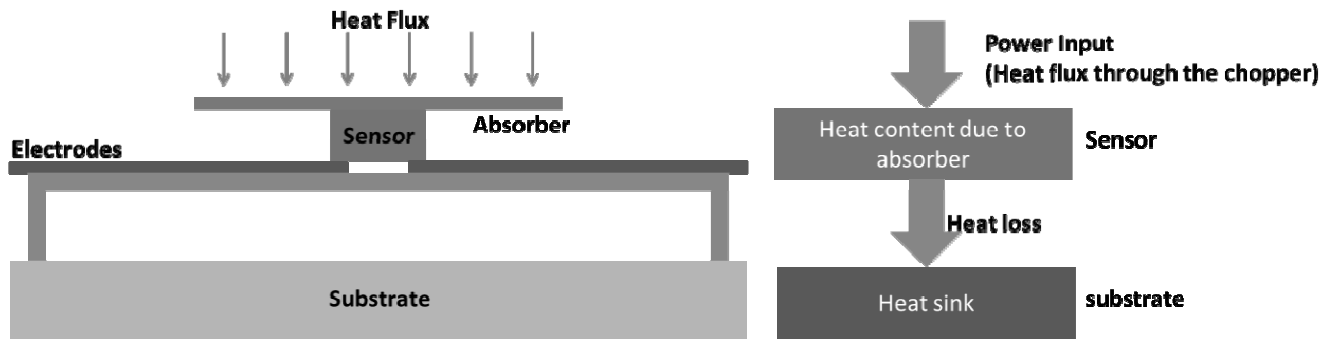


Figure 1. Heat transfer process of a pyroelectric detector [3]

shows that G_{eff} must be low for larger ΔT . From (4), we can see that for pyroelectric detectors, the effective thermal conductance is due to mainly thermal conduction through the supporting structure of the thermometer. So, the thermal conductivity between the heat sink and thermometer must be made as low as possible. In this work, the aim was therefore set toward achieving lower thermal conductance.

II. METHOD

The goal of this work was to design an infrared detector having background limited detectivity, capable of operating in the long wavelength IR region (8-14 μm), at room temperature, without the need for cryogenic cooling. Thermal detectors are ideal for this effort since they can operate at room temperature and among them pyroelectric detector was selected since it does not require any bias current to operate and thus free of $1/f$ -noise. For background limited performance, thermal noise can be neglected. In order to achieve high detectivity, it is important to reduce noise equivalent power (NEP), which can be achieved by ensuring lower noise and higher voltage responsivity. So, high IR absorption and low thermal conductance are vital for the detector performance. $\text{Ni}_{0.8}\text{Cr}_{0.2}$ was used as the absorber material due to its high absorption at infrared frequencies (8-14 μm).

The sensor and absorber layers were supported and separated from the substrate by a spider web structure designed with meandered struts, which helped in low conduction of heat energy from the sensor to the substrate as well as interface circuitry. The electrodes were also meandered to avoid heat loss. Fig. 2 shows top view of the design of spider web support along with the electrodes used in this work. Al_2O_3 was used as the spider web material since it has high yield strength (15.4 GPa), low thermal conductivity (0.25 W/cm/K), and high optical transmittance (~ 0.9). The

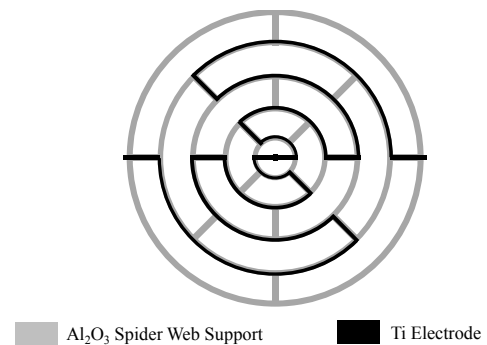


Figure 2. Geometry of the spider web support and electrodes

evolution of electron-beam lithography, nanoimprinting, and deep ultraviolet lithography has enabled sub-100nm features to be patterned. So, study of 50 to 100nm strut width was feasible. Ti was selected as the electrode material since it has relatively lower thermal conductivity of 0.219 W/cm/K along with high electrical conductivity of $4.2 \times 10^{-7} \Omega\text{-m}$.

Ca modified lead titanate was chosen as the pyroelectric material because of its good pyroelectric coefficient of $43 \times 10^{-9} \text{Ccm}^{-2}\text{K}^{-1}$ and figure of merit of $2340 \text{V cm}^{-2}\text{J}^{-1}$ [3]. A Si substrate was used because of its excellent electrical and mechanical properties.

Geometry of the structure is shown in Fig. 3. The design and analysis of the pyroelectric detector was done by using IntelliSuite[®] software. Several modules, for instance, IntelliMask, FabViewer, 3DBuilder, and Thermo Electro Mechanical (TEM) were used to design the photomasks of each layer and generate 3-D models, to perform the simulation by finite element analysis (FEM) method.

III. RESULT

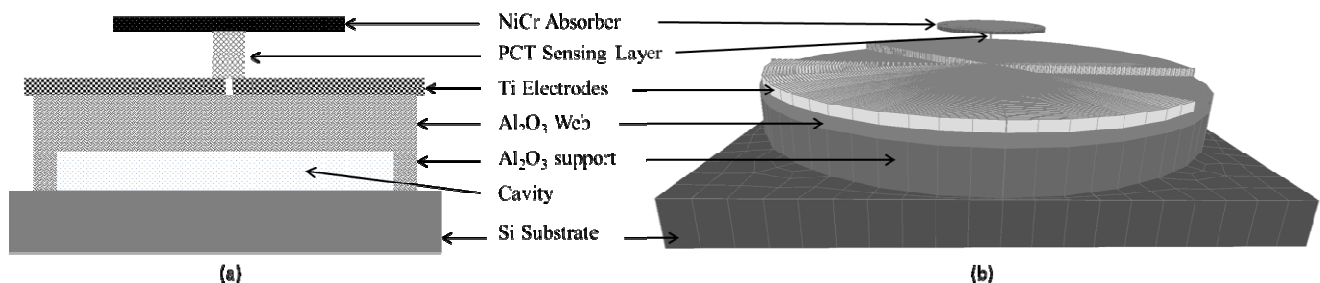
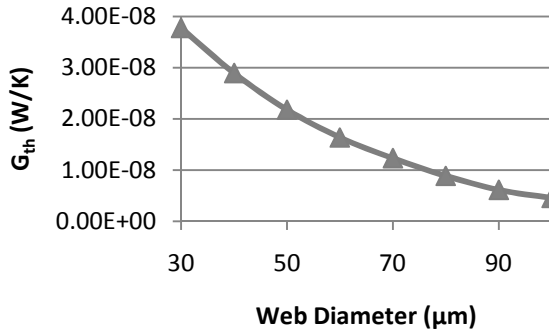


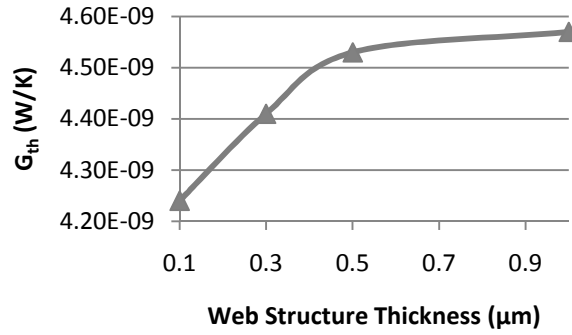
Figure 3. Geometry of the pyroelectric detector

The effects of strut number, thickness, dimension, and width of different layers on thermal conductance were studied.

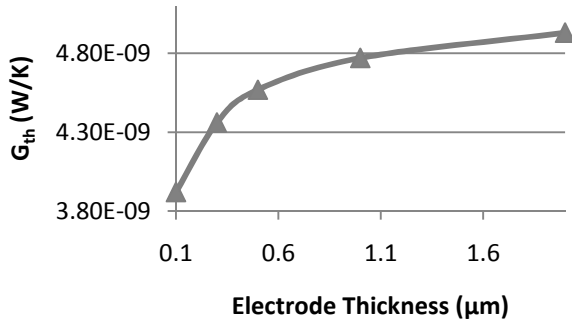
In this paper, we only report the variations of thermal conductance with respect to different parameters. Increasing



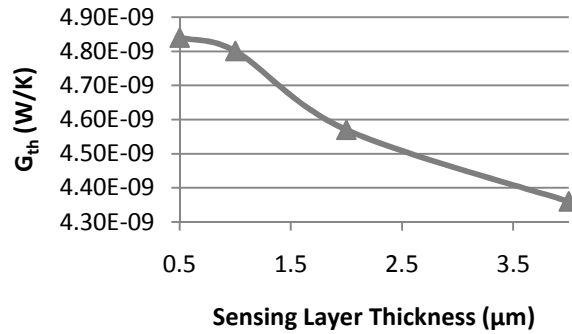
(a)



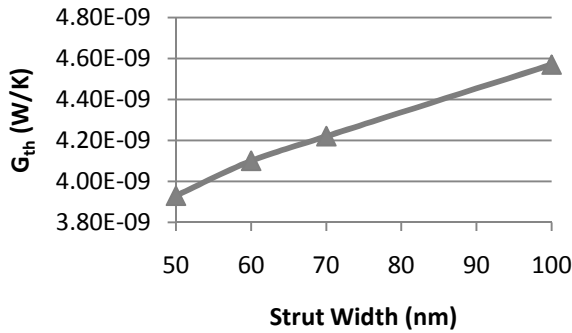
(b)



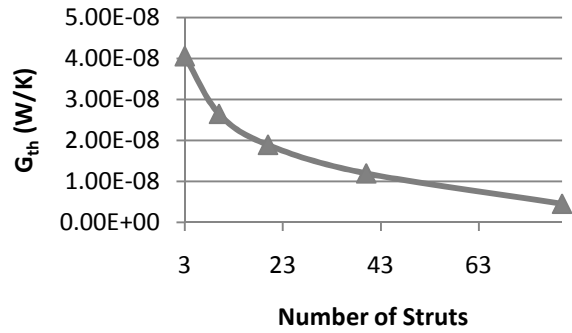
(c)



(d)



(e)



(f)

Figure 4. Effect of (a) web diameter, (b) web structure thickness, (c) electrode thickness, (d) sensing layer thickness, (e) strut width, and (f) number of struts on thermal conductance.

Thermal conductance of the structure was calculated from,

$$G_{th} = \frac{A_d}{\Delta T} I \quad (5)$$

Where, A_d is the area of the absorber and I is the intensity of the heat flux. Heat flux of $50 \text{ pW}/\mu\text{m}^2$ was applied on top of the absorber. The bottom of the substrate was kept fixed at 25°C or 298K which is the room temperature.

the dimension of the spider web structure led to lower thermal conductance as shown in Fig. 4(a). The thermal conductance for heat conduction process is related to the path length (L) according to the Fourier's law for heat conduction as,

$$G_{th} = \frac{A}{L} \kappa \quad (6)$$

Where, A is the area of the plane perpendicular to the direction of heat conduction and κ is the thermal conductivity of the material.

A larger web structure had a longer path length which caused lower thermal conductance. However, an increase in the web structure size means a bulkier detector. So it put a limit on this step.

Because of lower thermal resistance due to larger cross-sectional area of thicker web structure, as can be seen from (6), the device showed increasing thermal conductance with increase in thickness of web structure. This effect is shown in Fig. 4(b).

In the study of the effect of thickness of electrodes on thermal conductance (see Fig. 4(c)), it was found that thermal conductance was decreasing with decrease in electrode thickness. The reason behind this can be explained using (6). Smaller thickness led to smaller cross-sectional area which provided a higher thermal resistance for conductive heat to transfer.

A thicker sensing layer provides longer thermal path which helps in temperature rise. However, increase in thermal mass tends to increase thermal conductance. So, there was a race between these two factors and lower thermal conductance was found with increasing sensing layer thickness as demonstrated in Fig. 4(d).

Study of strut width showed that decreased width can provide lower thermal conductance (see Fig. 4(e)). Struts with smaller width have smaller cross-sectional area and thus

provide higher thermal resistance. Thus lower conduction can be planned.

It was observed that number of struts has a paramount effect on thermal conductance as shown in Fig. 4(f). Addition of struts provided longer thermal path length and hence reduced thermal conductance.

The thermal conductance between the sensor and the substrate (heat sink) was obtained as low as 4.57×10^{-9} W/K compared to the radiative thermal conductance of 3.69×10^{-7} W/K. Such low thermal conductivity will yield a high sensitivity detector.

ACKNOWLEDGMENT

This work was supported in part by National Science Foundation under Grants CREST HRD-0630388, CREST HRD-1242067 and NASA URC NNX09AU90A.

REFERENCES

- [1] A. Rogalski, "Infrared detectors: status and trends," *Progress in Quantum Electronics*, vol. 27, pp. 59-210, 2003.
- [2] A. Rogalski, "Infrared thermal detectors versus photon detectors: I. Pixel performance," *Material science and material properties for infrared optoelectronics, proceedings*, vol. 3182, pp. 14-25, 1997.
- [3] S. G. Porter, "A brief guide to pyroelectric detectors," *Ferroelectrics*, vol. 33, pp. 193-206, 1981.